CRYSTAL GROWTH & DESIGN

ARTICLE

pubs.acs.org/crystal

Unprecedented Tuning of Structures and Gas Sorption Properties of Two 2D Nickel Metal−Organic Frameworks via Altering the Positions of Fluorine Atoms in Azamacrocyclic Ligands

Xian-Rui Meng, Di-Chang Zhong, Long Jiang,* Huan-Yong Li, and Tong-Bu Lu*

MOE Key Laboratory of Bioinorganic and Synthetic Chemistry, State Key Laboratory of Optoelectronic Materials and Technologies, and School of Chemistry and Chemical Engineering, Sun Yat-Sen University, Guangzhou 510275, China

Supporting Information

ABSTRACT: Two 2D metal−organic frameworks (MOFs) of $[NiL^1]_3[BTC]_2\cdot 7H_2O\cdot 6DMF$ (**1**) and $[NiL^2]_3[BTC]_2\cdot H_2O\cdot 3DMF$ (**2**) have been constructed using macrocyclic Ni(II) complexes ($[NiL^1](ClO_4)_2$/$[NiL^2](ClO_4)_2$) and BTC^{3-} as building blocks [L^1 = 3,10-bis(4- fluorobenzyl)-1,3,5,8,10,12-hexaazacyclotetradecane, L^2 = 3,10-bis(2-fluorobenzyl)-1,3,5,8,10,12-hexaazacyclotetradecane, and BTC^{3-} = 1,3,5-benzenetricarboxylate]. The results of X-ray diffraction analyses indicate that **1** shows a 2D brick wall structure with BTC^{3-} bridging three $[NiL^1]^{2+}$ via C_1 symmetry, while **2** displays a 2D honeycomb-like structure with BTC^{3-} bridging three $[NiL^2]^{2+}$ via C_3 symmetry. The results of gas sorption measurements indicate that desolvated **1** can selectively adsorb CO_2 rather than N_2 and H_2, while desolvated **2** cannot adsorb any of these gases under the same condition. More interestingly, the sorption isotherm of CO_2 for desolvated **1** shows a large hysteresis. The different sorption properties of desolvated **1** and **2** can be attributed to their different structures tuned by the positions of the fluorine atoms in the macrocyclic ligands.

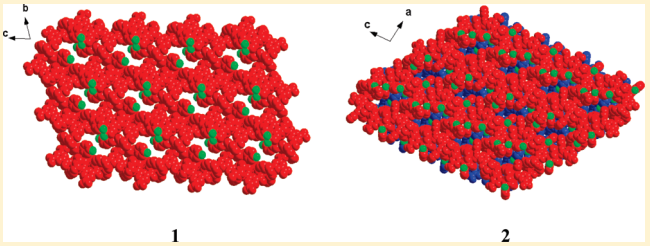

INTRODUCTION

The rational design and construction of metal−organic frameworks (MOFs) with fascinating structures and functions have achieved great progress over the past two decades,[1−4] while control synthesis of MOFs with desired structures and properties is still a great challenge. Many efforts have been made to control the structures and properties, of which modification of organic ligands with different substituents is a comparatively effective strategy. Up to now, a number of investigations in this aspect have been reported.[5−7] For example, Chen and co-workers have demonstrated that simple modifications of imidazolate ligand with a methyl or ethyl substituent at the 2-position can tune the orientation of adjacent metal coordination polyhedra to produce new MOFs with different structures and properties.[7c] Lang et al. found that modifications of 1,3-benzenedicarboxylate with different substituted R groups (OH, COOH, NO_2, and Me) at the 5-position can afford four different MOFs.[6a] However, reports on tuning structures and properties of MOFs by modifying the ligands with the same substituent in different positions are rare.[8]

Macrocyclic complexes are usually employed as useful building blocks for the constructions of novel MOFs, as they can provide fixed numbers of vacant coordination sites at the fixed positions and enable the extending direction of the network to be controllable.[9] To date, lots of macrocyclic ligands based MOFs with unique properties have been reported.[10−13] In this paper, we report the synthesis, crystal structures, and gas sorption properties of two two-dimensional (2D) MOFs of $[(NiL^1)_3(BTC)_2]\cdot 6DMF\cdot 7H_2O$ (**1**) and $[(NiL^2)_3(BTC)_2]\cdot 3DMF\cdot H_2O$ (**2**) (L^1 = 3,10-bis(4-fluorobenzyl)-1,3,5,8,10,12-hexaazacyclo-tetradecane, L^2 = 3,10-bis(2- fluorobenzyl)-1,3,5,8,10,12-hexaazacyclotetradecane, and BTC^{3-} = 1,3,5-benzenetricarboxylate; Scheme 1). It is interesting to note that although **1** and **2** were synthesized under the same condition, they exhibit different structures and adsorption behaviors, which can be ascribed to the different positions of the fluorine atoms in the macrocyclic ligands.

EXPERIMENTAL SECTION

Na_3BTC was prepared by the reaction of H_3BTC with an aqueous solution of NaOH.[13b] $[NiL^1](ClO_4)_2$ and $[NiL^2](ClO_4)_2$ were prepared according to the previously reported methods.[14] All of the other chemicals are commercially available and used without further purification. Elemental analyses were determined using Elementar Vario EL elemental analyzer. The IR spectra were recorded in the 4000−400 cm^{-1} region using KBr pellets and a Bruker EQUINOX 55 spectrometer. TG analyses were performed on a Netzsch TG 209 instrument under nitrogen atmosphere, with a heating rate of 10 °C/min. Variable-temperature powder X-ray diffraction measurements were performed on a Bruker D8 ADVANCE X-ray diffractometer.

Received: February 15, 2011
Revised: March 8, 2011
Published: April 01, 2011

Scheme 1. Structures of Two Ni(II) Macrocyclic Ligands with the Fluorine Substituent at Different Positions

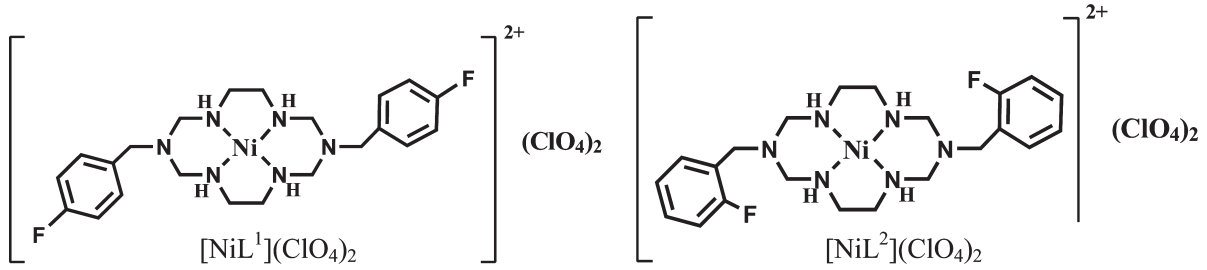

Table 1. Crystal Data and Structure Refinements for 1 and 2

	1	2
formula	$C_{102}H_{158}O_{25}N_{24}F_6Ni_3$	$C_{93}H_{125}O_{16}N_{21}F_6Ni_3$
F_w	2410.65	2083.27
temperature (K)	123(2)	123(2)
crystal system	triclinic	triclinic
space group	$P\bar{1}$	$P\bar{1}$
crystal size (mm^3)	0.40 × 0.33 × 0.31	0.37× 0.31 × 0.28
a (Å)	10.3512(16)	16.5659(6)
b (Å)	16.2520(15)	17.3791(5)
c (Å)	19.239(2)	18.8432(6)
α (°)	72.012(9)	112.489(3)
β (°)	82.716(11)	92.471(3)
γ (°)	72.597(11)	102.115(3)
V (Å ^{3})	2935.3(6)	4854.8(3)
Z/D_c (g cm^{-3})/μ (mm^{-1})	1/1.364/1.305	2/1.425/1.409
max/min transmission	0.688/0.623	0.694/0.624
reflns collected	23390	34157
unique reflns. (R_{int})	8193 (0.0359)	14739 (0.0261)
GOF	1.051	1.052
R_1,[a] wR_2[b] [$I > 2\sigma(I)$]	0.0893, 0.2258	0.0418, 0.1181
R_1,[a] wR_2[b] (all data)	0.1328, 0.2553	0.0496, 0.1221

[a] $R_1 = \Sigma||F_o| - |F_c||/\Sigma|F_o|$. [b] $wR_2 = [\Sigma[w(F_o^2 - F_c^2)^2]/\Sigma w(F_o^2)^2]^{1/2}$, where $w = 1/[\sigma^2(F_o)^2 + (aP)^2 + bP]$ and $P = (F_o^2 + 2F_c^2)/3$.

Caution! Perchlorate salts of metal complexes with organic ligands are potentially explosive. They should be handled with care and prepared only in small quantities.

$[(NiL^1)_3(BTC)_2]\cdot 7H_2O\cdot 6DMF$ (1). An aqueous solution (3 mL) of Na_3BTC (0.018 g, 0.066 mmol) was layered with a dimethyl formamide (DMF) solution (4 mL) of $[NiL^1](ClO_4)_2$ (0.067 g, 0.1 mmol) at room temperature. After about 10 days, pink crystals suitable for X-ray analysis formed. Yield, 19 mg, 23% based on $[NiL^1](ClO_4)_2$. Anal. calcd for $C_{102}H_{158}O_{25}N_{24}F_6Ni_3$: C, 50.82; H, 6.61; N, 13.95. Found: C, 50.90; H, 6.52; N, 13.82%. IR (KBr pellet, cm^{-1}): 3399 (w), 3269 (w), 3215(w), 3145 (m), 2925 (s), 2867 (s), 1607 (vs), 1563 (vs), 1510 (vs), 1427(s),1354 (vs), 1270(m), 1226 (s), 1158(w), 1074 (m), 1023 (s), 924 (m), 858(m), 771(m), 715 (w), 421(w).

$[(NiL^2)_3(BTC)_2]\cdot H_2O\cdot 3DMF$ (2). Pink crystals of **2** were obtained by a similar procedure to that of **1** except using $[NiL^2](ClO_4)_2$ instead of $[NiL^1](ClO_4)_2$. Yield, 17 mg, 25% based on $[NiL^2](ClO_4)_2$. Anal. calcd for $C_{93}H_{125}O_{16}N_{21}F_6Ni_3$: C, 53.62; H, 6.05; N, 14.12. Found: C, 53.11; H, 6.11; N, 13.82%. IR (KBr pellet, cm^{-1}): 3403 (s), 3253 (s), 3196 (s), 3066 (w), 2928 (m), 2872 (s), 2778 (w), 1672 (vs), 1594 (vs), 1510 (vs), 1384 (vs), 1220 (s), 1157 (m), 1076 (m), 1020 (s), 990 (s), 856 (s), 771 (s), 420 (m).

X-ray Structure Determination. Single-crystal X-ray diffraction data for **1** and **2** were collected at 123 K on an Oxford Gemini S Ultra diffractometer with the Enhance X-ray Source of Cu radiation (λ = 1.54178 Å). All empirical absorption corrections were applied using spherical harmonics implemented in SCALE3 ABSPACK scaling algorithm.[15] The structures were solved by heavy atom methods, which yielded the positions of all nonhydrogen atoms. These were refined first isotropically and then anisotropically. The positional disorder of fluorobenzyl group and DMF molecules in **1** were treated with FVAR [the disordered components have been refined with occupancies of 0.627(11) and 0.373(11) for fluorobenzyl group, 0.662(13) and 0.338(13) for O8 atom in DMF molecule, and 0.25:0.30:0.45 for another disordered DMF molecule]. In **2**, the positional disorder was treated with half and 0.737(10):0.263(10) occupancies for disordered fluorine atom and DMF molecule, respectively. All of the disordered parts were restrained using DFIX, DELU, and SIMU instructions to make the displacement parameters more reasonable. All of the hydrogen atoms of the ligands were placed in calculated positions with fixed isotropic thermal parameters and included in the structure factor calculations in the final stage of full-matrix least-squares refinement. The hydrogen atoms of water molecules in **1** and **2** were assigned in the difference Fourier maps and refined isotropically. All calculations were performed using the SHELXTL system of computer programs.[16] The crystallographic data for **1** and **2** are summarized in Table 1, and the selected bond lengths and angles are listed in Table S1 in the Supporting Information.

Gas Sorption Measurements. N_2 and H_2 sorption measurements were performed using a Micromeritics ASAP 2020 instrument, and the CO_2 sorption measurements were carried out on a BELSORP-max automatic volumetric adsorption apparatus. All of the adsorption isotherms were collected in a relative pressure range from 10^{-4} to 1.0 atm. The cryogenic temperatures of 77 K required for N_2 and H_2 sorption measurements were controlled by liquid nitrogen, and the 195 K required for CO_2 sorption measurements was controlled using a dry ice−acetone bath. The initial outgassing process for the sample was carried out under a high vacuum (less than 10^{-6} mbar) at 110 °C for 10 h. The degassed sample and sample tube were weighed precisely and transferred to the analyzer.

RESULTS AND DISCUSSION

Crystal Structures. As shown in Figure 1a, the asymmetric unit of **1** contains three independent Ni(II) ions, in which each Ni(II) resides in an inversion center and coordinates with four N atoms from L^1 and two carboxylate O atoms from two individual BTC^{3-} anions, forming a slightly distorted octahedral geometry. The Ni−O distances [2.095(4) ∼ 2.161(4) Å] in axial positions are slightly longer than the Ni−N distances [2.051(6) ∼ 2.085(5) Å] in the equatorial plane (Table S1 in the Supporting Information). Along the bc plane, each BTC^{3-} anion bridges

dx.doi.org/10.1021/cg2002157 |Cryst. Growth Des. 2011, 11, 2020–2025

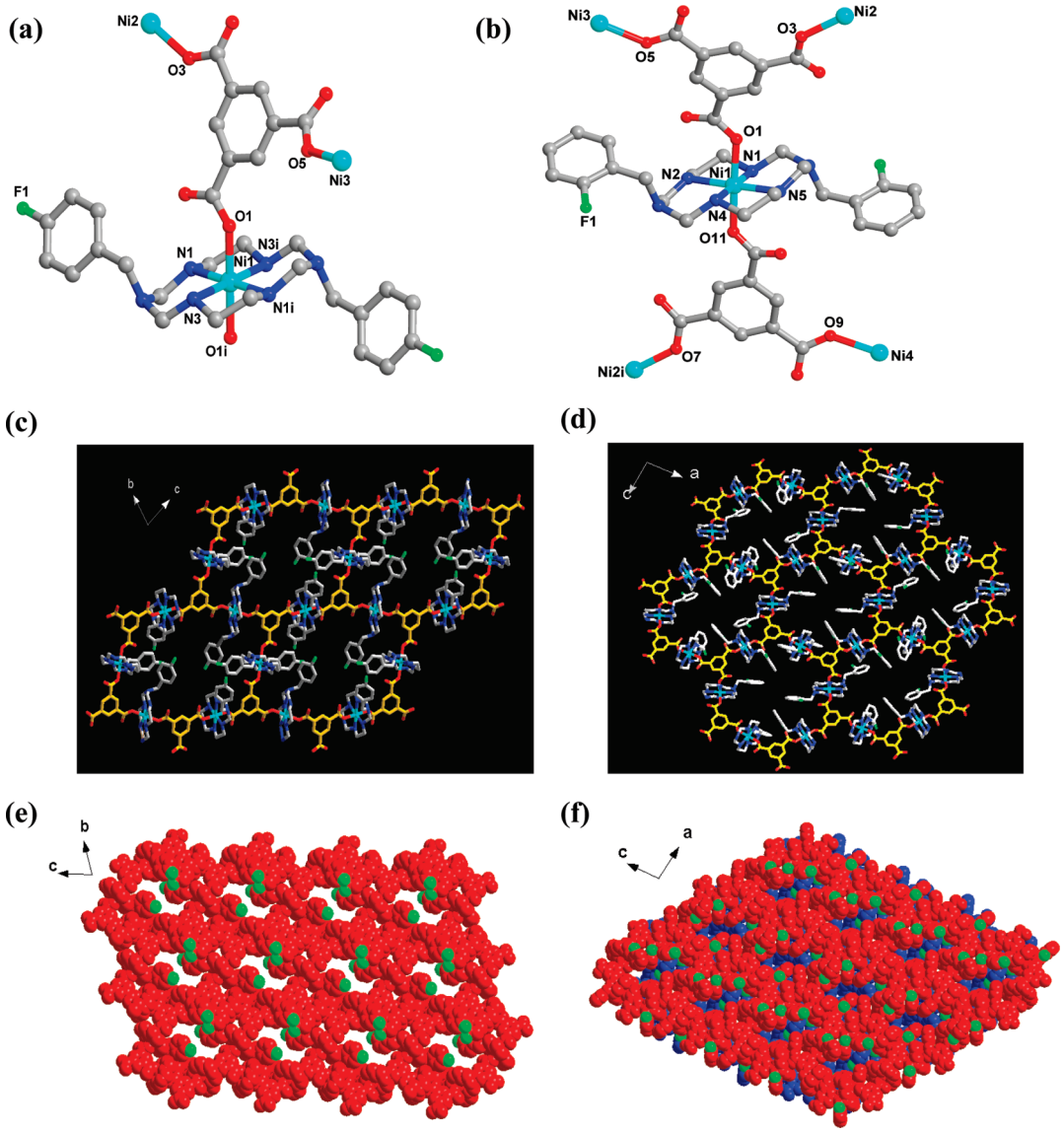

Figure 1. (a) Coordination environments of Ni(II) and the coordination mode of BTC^{3-} with C_1 symmetry in **1** [symmetric code: (i) $1 - x, -y, -z$]. Selected bond distances: Ni(1)−O(1), 2.129(4); Ni(2)−O(3), 2.095(4); and Ni(3)−O(5), 2.161(4) Å. (b) The coordination environments of Ni(II) and the coordination mode of BTC^{3-} with C_3 symmetry in **2** [symmetric code: (i) $x, -1 + y, -1 + z$]. Selected bond distances: Ni(1)−O(1), 2.1068(18); Ni(1)−O(11), 2.1435(18); Ni(2)−O(3), 2.1203(17); Ni(2i)−O(7), 2.1203(17); Ni(3)−O(5), 2.1085(17); and Ni(4)−O(9), 2.1219(16) Å. (c) Two-dimensional brick wall structure in **1**. (d) Two-dimensional honeycomb-like structure in **2**. (e) The space-filling model of 3D framework with 1D channels in **1**. (f) The space-filling model of 3D nonporous framework in **2**.

three $[NiL^1]^{2+}$ through C_1 symmetry to generate a 2D layer with brick wall structure (Figure 1c). The adjacent 2D layers are further connected through interlayer hydrogen-bonding interactions between the guest DMF and water molecules, secondary amines of L^1, and uncoordinated carboxylate oxygen atoms of BTC^{3-} (see Figure S1 in the Supporting Information), forming a three-dimensional (3D) network structure. Such a packing pattern results in one-dimensional (1D) channels along the *a*-axis (Figure 1e), with the sizes of 4.2 Å × 3.2 Å. It should be noted that all of the fluorine atoms in L^1 point to the channel, resulting in a fluorine-decorated surface (Figure 1e). DMF and water molecules are filled in the channels, and about 35.2% solvent-accessible volume is estimated by using PLATON program.[17]

In contrast to **1**, the asymmetric unit of **2** contains four independent Ni(II) ions, in which Ni3 and Ni4 lie on an inversion center. As shown in Figure 1b, each Ni(II) ion shows a distorted N_4O_2 octahedral geometry, with four N atoms from L^2 in the equatorial plane and two O atoms from two BTC^{3-} anions at axial positions. Each BTC^{3-} anion bridges three Ni(II) ions through a C_3 symmetry. By the bridging of BTC^{3-} anions, $[NiL^2]^{2+}$ cations are connected together to generate a 2D honeycomb-like layer (Figure 1d), and the fluorine atoms point out of the layer. In contrast to **1**, the fluorine atoms in **2** do not reside in the cavities; they form C−H···F hydrogen bonds with the hydrogen atoms of L^2 in the adjacent layers [F1···C34 = 3.084(3), F1···C35 = 3.049(3), F2···C23 = 3.058(4), and F2···C24 = 3.136 (4) Å] (Figure S2 in the Supporting Information). This packing mode leads to the cavities of 2D honeycomb-like layer being blocked by the adjacent layers, resulting in a nonporous 3D framework (Figure 1f).

dx.doi.org/10.1021/cg2002157 |*Cryst. Growth Des.* 2011, 11, 2020–2025

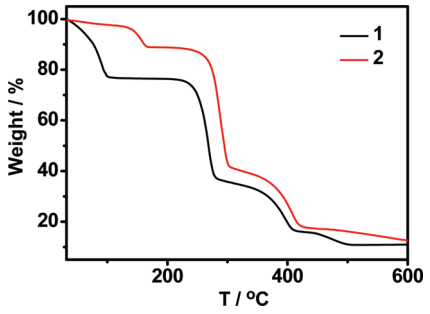

Figure 2. TG curves of **1** and **2**.

It is interesting to note that the different positions of the fluorine atoms in the macrocyclic ligands can tune the structures of **1** and **2**. The fluorine atoms at the 4-poition in L^1 point to the cavities of 2D brick wall layer, and they do not participate the hydrogen bond formation, and 2D brick wall layers are packed in a parallel way, resulting in the formation of **1** with 1D channels. The fluorine atoms at the 2-position in the L^2 form interlayer hydrogen bonds with the hydrogen atoms of L^2 in adjacent layers, and the cavities of 2D honeycomb-like layer are blocked by the adjacent layers, resulting in a nonporous 3D framework of **2**.

Thermal Behavior. To evaluate the stability of **1** and **2**, TG analyses and variable XRD measurements were carried out. The TGA curve of **1** shows a weight loss of 23.5% from room temperature to 135 °C, corresponding to the removal of six DMF and seven water molecules (calcd 23.4%). The desolvated compound is stable up to 250 °C, followed by another three steps of weight losses after that temperature (Figure 2). For **2**, the observed weight loss of 11.3% in the temperature range of 32−180 °C is close to the losses of one water and three DMF molecules (calcd 11.5%). The framework is stable up to 260 °C and then begins to decompose upon further heating (Figure 2).

The variable-temperature XRD patterns for **1** and **2** were recorded from 30 to 300 °C under air atmosphere. The results show that the patterns of **1** and **2** were changed when the samples were heated over 50 and 90 °C, respectively (Figure 3). This may be attributed to the slide between layers after the losses of guest molecules. The frameworks of **1** and **2** can be stable up to 240 °C, which are consistent with the results of TG analyses.

Sorption Properties. Considering some 2D MOFs exhibit good CO_2 adsorption ability,[18] we performed the gas sorption measurements for desolvated **1** (**1d**) and **2** (**2d**). The CO_2, N_2, and H_2 sorption measurements were carried out in a relative pressure range from 10^{-4} to 1 atm, indicating that **1d** can selectively adsorb CO_2 over N_2 and H_2, and **2d** cannot adsorb any type of gas under the same condition. The selective CO_2 adsorption over the other gases for **1d** can be ascribed to the quadrupole moment of CO_2 (-1.4×10^{-39} C m^2),[10a,21] which induces interaction with the framework to open up the channels.[10b] The interacting sites of CO_2 with the interior of **1d** may be the F atoms and/or the secondary amines of L^1 located at the surface of the pores.

As shown in Figure 4, the adsorption isotherm of CO_2 at 195 K for **1d** shows two-step sorption. From 0 to 0.47 atm, **1d** can only capture 8.5 mL (0.38 mmol/g, STP) of CO_2, and then, it starts to jumpily adsorb CO_2 and gradually reaches 59.7 mL (2.66 mmol/g, STP) at 1 atm. More interestingly, the desorption isotherm, also showing two-step sorption, does not retrace the adsorption

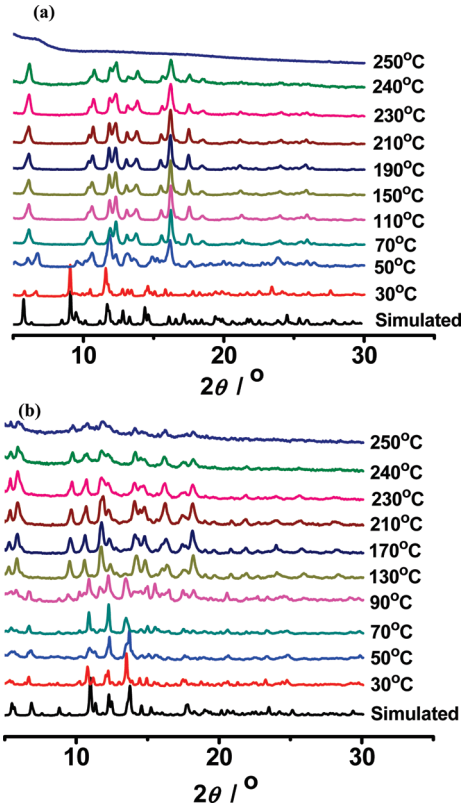

Figure 3. Variable-temperature XRD patterns for **1** (a) and **2** (b).

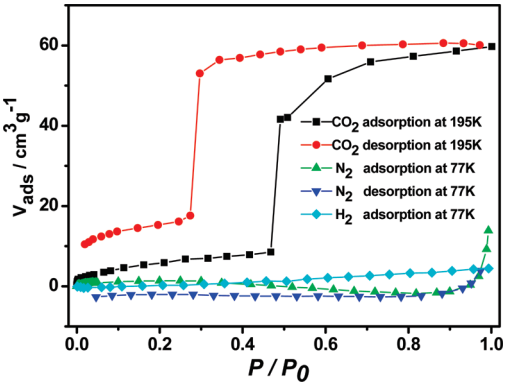

Figure 4. Sorption isotherms of N_2, CO_2, and H_2 for **1d**.

isotherm. From 1.0 to 0.30 atm, only 11.7% adsorbed CO_2 was desorbed, following an abrupt desorption, resulting in a large hysteresis. The stepwise and hysteretic behaviors of CO_2 sorption observed in MOFs can be described as "breathing effect"[19] or "gate effect".[20] At lower pressure, the distance between adjacent layers becomes very near after the removal of guest molecules; thus, the amount of adsorption is quite small. However, once the limited porous volumes are fully filled with CO_2 molecules, further adsorbed CO_2 molecules can expand the interlayer distance to allow more CO_2 molecules to enter. The large hysteretic behavior of CO_2 sorption can be ascribed to the presence of F atoms and/or the secondary amines of L^1 located at the surface of the pores, which can strongly interact with CO_2 molecules, and this strong interaction leads to the generation of

dx.doi.org/10.1021/cg2002157 |*Cryst. Growth Des.* 2011, 11, 2020–2025

large hysteresis.[10b,18b,22] Although the sorption capacity of **1d** for CO_2 is not as great as those of other reported MOFs,[10b] the high sorption selectivity and large hysteresis suggest that **1d** is potential for the application of CO_2 separation and storage.

CONCLUSION

Two 2D MOFs of **1** and **2** were synthesized under the same reaction condition. Interestingly, altering the positions of fluorine atoms in the macrocyclic ligands lead to these two MOFs exhibiting different structures and gas adsorption behaviors. Compound **1** shows a 2D brick wall structure with 1D open channels, while **2** displays a 2D honeycomb-like structure without pores. The desolvated **1** can selectively adsorb CO_2 rather than N_2 and H_2 and displays a stepwise adsorption process and large hysteretic behavior, while the desolvated **2** has no adsorption for any of these gases. The result presented here demonstrates that altering the positions of the substituent group in the macrocyclic ligand is an effective strategy for tuning the structures and properties in the rational design of MOFs as functional materials.

ASSOCIATED CONTENT

Supporting Information. X-ray crystallographic file in CIF format, the selected bond distances and angles, the figures of interlayer hydrogen-bonding interactions in **1** and **2**. This material is available free of charge via the Internet at http://pubs.acs.org.

AUTHOR INFORMATION

Corresponding Author

*Fax: +86-20-84112921. E-mail: jianlonchem@yahoo.com.cn (L.J.) and lutongbu@mail.sysu.edu.cn (T.-B.L.).

ACKNOWLEDGMENT

This work was supported by NSFC (20625103 and 20831005), 973 Program of China (2007CB815305), and Sun Yat-Sen University Science Foundation.

REFERENCES

(1) (a) Schroder, M., Ed. *Functional Metal-Organic Frameworks: Gas Storage, Separation and Catalysis*; Springer: New York, 2010. (b) MacGillivray, L. R., Ed. *Metal-Organic Frameworks: Design and Application*; Wiley: Hoboken, NJ, 2010. (c) Hong, M.-C., Chen, L., Eds. *Design and Construction of Coordination Polymers*; Wiley: Hoboken, NJ, 2009. (d) Tranchemontagne, D. J.; Mendoza-Cortes, J. L.; O'Keeffe, M. O.; Yaghi, M. *Chem. Soc. Rev.* **2009**, *38*, 1257.(e) Kirillov, A. M. *Coord. Chem. Rev.* **2011**, http://dx.doi.org/10.1016/j.ccr.2011.01.023. (f) Perry, J. J.; Perman, J. A.; Zaworotko, M. J. *Chem. Soc. Rev.* **2009**, *38*, 1400. (g) Qiu, S. L.; Zhu, G. S. *Coord. Chem. Rev.* **2009**, *253*, 2891.

(2) (a) Ma, L. F.; Wang, L. Y.; Huo, X. K.; Wang, Y. Y.; Fan, Y. T.; Wang, J. G.; Chen, S. H. *Cryst. Growth Des.* **2008**, *8*, 620. (b) Ma, L. F.; Wang, Y. Y.; Wang, L. Y.; Liu, J. Q.; Wu, Y. P.; Wang, J. G.; Shi, Q. Z.; Peng, S. M. *Eur. J. Inorg. Chem.* **2008**, 693. (c) Zheng, G. L.; Ma, J. F.; Su, Z. M.; Yan, L. K.; Yang, J.; Li, Y. Y.; Liu, J. F. *Angew. Chem., Int. Ed.* **2004**, *43*, 2409. (d) Pan, L.; Adams, K. M.; Hernandez, H. E.; Wang, X. T.; Zheng, C.; Hattori, Y.; Kaneko, K. *J. Am. Chem. Soc.* **2003**, *125*, 3062. (e) Eddaoudi, M.; Kim, J.; Rosi, N.; Vodak, D.; Wachter, J.; O'Keeffe, M.; Yaghi, O. M. *Science* **2002**, *295*, 469.

(3) (a) Férey, G.; Millange, F.; Morcrette, M.; Serre, C.; Doublet, M. L.; Greneche, J. M.; Tarascon, J. M. *Angew. Chem., Int. Ed.* **2007**, *46*, 3259. (b) Zhang, L. Y.; Zhang, J. P.; Lin, Y. Y.; Chen, X. M. *Cryst. Growth Des.* **2006**, *6*, 1684. (c) Fang, Q.; Zhu, G.; Xue, M.; Sun, J.; Sun, F.; Qiu, S. *Inorg. Chem.* **2006**, *45*, 3582. (d) Han, Z. B.; Cheng, X. N.; Chen, X. M. *Cryst. Growth Des.* **2005**, *5*, 695.

(4) (a) Gao, X. M.; Li, D. S.; Wang, J. J.; Fu, F.; Wu, Y. P.; Hu, H. M.; Wang, J. W. *CrystEngComm* **2008**, 479. (b) Biradha, K.; Sarkar, M.; Rajput, L. *Chem. Commun.* **2006**, 4169. (c) Zheng, G. L.; Ma, J. F.; Yang, J.; Li, Y. Y.; Hao, X. R. *Chem.—Eur. J.* **2004**, *10*, 3761. (d) Ma, J. F.; Yang, J.; Zheng, G. L.; Li, L.; Liu, J. F. *Inorg. Chem.* **2003**, *42*, 7531.

(5) (a) Ren, H.; Song, T. Y.; Xu, J. N.; Jing, S. B.; Yu, Y.; Zhang, P.; Zhang, L. R. *Cryst. Growth Des.* **2009**, *9*, 105. (b) Du, M.; Zhang, Z. H.; You, Y. P.; Zhao, X. J. *CrystEngComm* **2008**, 306. (c) Li, X. J.; Cao, R.; Guo, Z. G.; Li, Y. F.; Zhu, X. D. *Polyhedron* **2007**, *26*, 3911. (d) Oh, M.; Carpenter, G. B.; Sweigart, D. A. *Organometallics* **2003**, *22*, 2364.

(6) (a) Liu, D.; Li, H. X.; Liu, L. L.; Wang, H. M.; Li, N. Y.; Ren, Z. G.; Lang, J. P. *CrystEngComm* **2010**, *12*, 3708. (b) Ma, L. F.; Wang, L. Y.; Wang, Y. Y.; Du, M.; Wang, J. G. *CrystEngComm* **2009**, *11*, 109. (c) Zhou, D. S.; Wang, F. K.; Yang, S. Y.; Xie, Z. X.; Huang, R. B. *CrystEngComm* **2009**, *11*, 2548. (d) Li, S. L.; Lan, Y. Q.; Ma, J. C.; Ma, J. F.; Su, Z. M. *Cryst. Growth Des.* **2010**, *10*, 1161.

(7) (a) Huang, X. C.; Zhang, J. P.; Chen, X. M. *J. Am. Chem. Soc.* **2004**, *126*, 13218. (b) Huang, X. C.; Zhang, J. P.; Lin, Y. Y.; Chen, X. M. *Chem. Commun.* **2005**, 2232. (c) Huang, X. C.; Lin, Y. Y.; Zhang, J. P.; Chen, X.-M. *Angew. Chem., Int. Ed.* **2006**, *45*, 1557.

(8) (a) Ma, L. F.; Wang, L. Y.; Chen, S. H.; Hou, H. W.; Battern, S. R. *Polyhedron* **2009**, *28*, 2494. (b) Ma, C. B.; Chen, C. N.; Liu, Q. T.; Liao, D. Z.; Li, L. C.; Sun, L. C. *New J. Chem.* **2003**, *27*, 890. (c) Zhang, H. X.; Kang, B. S.; Xu, A. W.; Chen, Z. N.; Zhou, Z. Y.; Chan, A. S. C.; Yu, K. B.; Ren, C. *J. Chem. Soc., Dalton Trans.* **2001**, *18*, 2559.

(9) Suh, M. P.; Cheon, Y. E.; Lee, E. Y. *Coord. Chem. Rev.* **2008**, *252*, 1007.

(10) (a) Park, H. J.; Suh, M. P. *Chem. Commun.* **2010**, 610. (b) Choi, H. S.; Suh, M. P. *Angew. Chem., Int. Ed.* **2009**, *48*, 6865. (c) Moon, H. R.; Kim, J. H.; Suh, M. P. *Angew. Chem., Int. Ed.* **2005**, *44*, 1261. (d) Lee, E. Y.; Suh, M. P. *Angew. Chem., Int. Ed.* **2004**, *43*, 2798.

(11) (a) Choi, H. J.; Suh, M. P. *J. Am. Chem. Soc.* **2004**, *126*, 15844. (b) Suh, M. P.; Ko, J. W.; Choi, H. J. *J. Am. Chem. Soc.* **2002**, *124*, 10976. (c) Choi, H. J.; Lee, T. S.; Suh, M. P. *J. Inclusion Phenom. Macrocyclic Chem.* **2001**, *41*, 155. (d) Choi, H. J.; Lee, T. S.; Suh, M. P. *Angew. Chem., Int. Ed.* **1999**, *38*, 1405.

(12) (a) Cheon, Y. E.; Suh, M. P. *Chem.—Eur. J.* **2008**, *14*, 3961. (b) Suh, M. P.; Moon, H. R.; Lee, E. Y.; Jang, S. Y. *J. Am. Chem. Soc.* **2006**, *128*, 4710. (c) Suh, M. P.; Cheon, Y. E. *Aust. J. Chem.* **2006**, *59*, 605.

(13) (a) Lu, T. B.; Ou, G. C.; Jiang, L.; Feng, X. L.; Ji, L. N. *Inorg. Chim. Acta* **2005**, *358*, 3241. (b) Lu, T. B.; Xiang, H.; Luck, R. L.; Jiang, L.; Mao, Z. W.; Ji, L. N. *New J. Chem.* **2002**, *26*, 969. (c) Lu, T. B.; Xiang, H.; Su, C. Y.; Cheng, P.; Mao, Z. W.; Ji, L. N. *New J. Chem.* **2001**, *25*, 216.

(14) (a) Ou, G.-C.; Jiang, L.; Feng, X.-L.; Lu, T.-B. *Inorg. Chem.* **2008**, *47*, 2710. (b) Jiang, L.; Feng, X.-L.; Lu, T.-B. *Cryst. Growth Des.* **2005**, *5*, 1469.

(15) *CrysAlis RED*, Version 1.171.31.7; Oxford Diffraction Ltd.: 2006.

(16) Sheldrick, G. M. *SHELXS 97, Program for Crystal Structure Refinement*; University of Göttingen: Göttingen, 1997.

(17) Spek, A. L. *PLATON A Multipurpose Crystallographic Tool*; Utrecht University: Utrecht, 2007.

(18) (a) Maji, T. K.; Kitagawa, S. *Pure Appl. Chem.* **2007**, *79*, 2155. (b) Férey, G.; Mellot-Draznieks, C.; Serre, C.; Millange, F. *Acc. Chem. Res.* **2005**, *38*, 217. (c) Millward, A. R.; Yaghi, O. M. *J. Am. Chem. Soc.* **2005**, *127*, 17998. (d) Kitagawa, S.; Uemura, K. *Chem. Soc. Rev.* **2005**, *34*, 109. (e) Yaghi, O. M.; O'Keeffe, M.; Ockwig, N. W.; Chae, H. K.; Eddaoudi, M.; Kim, J. *Nature* **2003**, *423*, 705. (f) Kitagawa, S.; Kondo, M. *Bull. Chem. Soc. Jpn.* **1998**, *71*, 1737.

(19) Bourrelly, S.; Llewellyn, P. L.; Serre, C.; Millange, F.; Loiseau, T.; Férey, G. *J. Am. Chem. Soc.* **2005**, *127*, 13519.

(20) Li, D.; Kaneko, K. *Chem. Phys. Lett.* **2001**, *335*, 50.

(21) (a) Couck, S.; Denayer, J. M.; Baron, G. V.; Remy, T.; Gascon, J.; Kapteijin, F. *J. Am. Chem. Soc.* **2009**, *131*, 6326. (b) Bae, Y. S.;

Farha, O. K.; Spokoyny, A. M.; Mirkin, C. A.; Hupp, J. T.; Snurr, R. Q. *Chem. Commun.* **2008**, 4135. (c) Bastin, L.; Brcia, P. S.; Hurtado, E. J.; Silva, J. C.; Rodrigues, A. E.; Chen, B. *J. Phys. Chem.* **2008**, *112*, 1575. (d) Llewellyn, P. L.; Bourrelly, S.; Serre, C.; Filinchuk, Y.; Férey, G. *Angew. Chem., Int. Ed.* **2006**, *45*, 7751.

(22) (a) Férey, G.; Serre, C. *Chem. Soc. Rev.* **2009**, *38*, 1380. (b) Seo, J.; Sakamoto, R. H.; Bonneau, C.; Kitagawa, S. *J. Am. Chem. Soc.* **2009**, *131*, 12792. (c) Tanaka, D.; Nakagawa, K.; Higuchi, M.; Horike, S.; Kubota, Y.; Kobayashi, T. C.; Takata, M.; Kitagawa, S. *Angew. Chem., Int. Ed.* **2008**, *47*, 3914. (d) Serre, C.; Mellot-Draznieks, C.; Surble, S.; Audebrand, N.; Filinchuk, Y.; Férey, G. *Science* **2007**, *315*, 1828. (e) Uemura, K.; Yamasaki, Y.; Komagawa, Y.; Tanaka, K.; Kita, H. *Angew. Chem., Int. Ed.* **2007**, *46*, 6662.